

Hydrodynamical Simulations of the Solar Dynamo

Axel Brandenburg

HAO/NCAR*, P.O. Box 3000, Boulder, CO 80307-3000, USA

Abstract: Hydrodynamic simulations of the solar convection zone can be used to model the generation of differential rotation and magnetic fields, and to determine mean-field transport coefficients that are needed in mean-field models. The importance of the overshoot layer beneath the solar convection zone is discussed: it is the place where the magnetic field accumulates, although most of the field regeneration can still occur in the convection zone proper. We also discuss how systematically oriented bipolar regions can emerge from the convection zone where the magnetic field is highly intermittent.

1 Introduction

The engine driving solar and stellar activity is the dynamo. In theories of the solar corona and solar wind the dynamo magnetic fields are an important input quantity. In order to compute the loss of angular momentum during the evolution of the Sun we need to know the magnetic field strength as a function of the angular velocity. Properties of differential rotation and magnetic field geometry are bound to change during this complicated evolutionary process which can only be understood using detailed and realistic dynamo models. Thus, a better understanding of the solar dynamo is essential.

At present it is not feasible to compute realistically in a direct simulation the evolution of magnetic fields and fluid turbulence, because of the large range of different time and length scales that are important. Therefore, one expects the mean-field approach to be well-suited to address certain questions of solar and stellar magnetism (e.g. Schmitt 1993). In this theory, nondiffusive contributions to the turbulent electromotive force and the Reynolds stress tensor are described by α - and Λ -effects, respectively. These effects are responsible for generating large scale magnetic fields and driving differential rotation (Krause & Rädler 1980, Rüdiger 1989). Progress has recently been made to derive the Rossby number dependence of α - and Λ -effects, as well as the turbulent magnetic diffusivity, the eddy viscosity, and the eddy conductivity (e.g. Rüdiger & Kitchatinov 1993, Küker et al. 1993).

* The National Center for Atmospheric Research is sponsored by the National Science Foundation

In the mean-field approach solutions are only found for long time and length scales. In spite of such simplifications, this approach is actually rather complicated compared to direct three-dimensional simulations, because there are so many different turbulent transport coefficients, and because they are nonlinear in the magnetic field strength and the angular velocity. However, since our knowledge of these dependencies is based on uncontrolled approximations, it is essential to confirm such results using direct simulations. The problem here is that the conditions under which the mean-field approach applies usually do not overlap with those accessible to direct simulations. This includes in particular the requirement of scale separation which is not satisfied in our simulations (and not even in the Sun!).

We first discuss some key issues of dynamo simulations, such as magnetic buoyancy and the formation of large scale fields and bipolar regions. Such simulations are used to evaluate α and its dependence on various parameters. Some recent progress in constructing solar mean-field dynamos is reported and finally the question of the seat of the dynamo is discussed.

2 Numerical Simulations

Using a numerical simulation of idealised turbulent compressible convection in a small box at reasonably high magnetic Reynolds number it has been possible to study properties of the dynamo process, the formation of magnetic flux tubes and the magnetic buoyancy associated with such flux tubes; see Nordlund et al. (1992) and Brandenburg et al. (1993a). In these simulations the magnetic field grows on a dynamical (turnover) time scale until saturation sets in and a statistically steady state is reached approximately. By splitting the Lorentz force $\mathbf{J} \times \mathbf{B}$ in the simulation into its various components, it has been demonstrated that both the magnetic pressure gradient force (magnetic buoyancy) and the tension force (component of $\mathbf{B} \cdot \nabla \mathbf{B}$ in the direction of \mathbf{B}) are unimportant for saturation (Nordlund et al. 1992). Thus, saturation is accomplished mainly by the curvature force that prevents the flux tubes from bending beyond a certain point.

There is a strong tendency for the magnetic field to be sucked by the concentrated convective downdrafts and subsequently advected downwards to the bottom of the convection zone (Brandenburg et al. 1991a). This raises the question whether it makes sense to consider magnetic flux tubes as passive objects subjected to the influence of magnetic buoyancy. On the other hand, the magnetic field in these simulations is not yet strong enough to produce highly buoyant flux tubes. Nevertheless, in the simulations mentioned above, the maximum magnetic field strength in the overshoot layer can be 2 to 8 times larger than the local value of the equipartition field strength, $B_{\text{eq}} = u_t(\mu_0 \rho)^{1/2}$, where μ_0 is the permeability, ρ the density, and u_t the rms-velocity of the turbulent motions.

What needs to be changed in the simulations to make the flux tubes more intense? First of all, magnetic flux tubes are rather small objects (at least in the simulations) and they eventually disappear due to dissipation. In the Sun, dissipation is much smaller than in simulations with a finite number of mesh points. Thus, flux tubes would live longer and there would then be more time for them to gain maximal field strength. Secondly, in the simulations the Mach number at the bottom

of the convection zone is still unrealistically large and the magnetic field energy is only 3-10% of the kinetic energy density, i.e.

$$v_A \ll u_t \ll c \quad (\text{in simulations}), \quad (1)$$

where $v_A = \langle B^2 / \mu_0 \rho \rangle^{1/2}$ is the Alfvén velocity, and c the speed of sound. At the bottom of the solar convection zone, the situation is probably more like

$$u_t \lesssim v_A \ll c \quad (\text{solar overshoot layer}). \quad (2)$$

Larger sound velocities and smaller Mach numbers (Ma) are automatically obtained by choosing the Rayleigh number (Ra) large enough. This may be demonstrated by solving the standard mixing length equations for the same setup used in numerical simulations of convection in an unstable layer with a stable layer beneath (Table 1). Here we define $\text{Ra Pr} = (gd^3/\bar{\chi}^2)(1 - \nabla_{\text{ad}}/\nabla_{\text{rad}})$, where g is gravity ($5 \cdot 10^4 \text{ cm/s}^2$), d the thickness of the unstable layer in the model (100 Mm), and $\bar{\chi}$ the mean radiative diffusion coefficient, which is varied in order to vary Ra. $\text{Pr} = \nu/\bar{\chi}$ is the Prandtl number.

Table 1. Turbulent velocity and Mach number at the bottom of the unstable layer for mixing length models with different Rayleigh number, but solar values for temperature and density. For $\text{Ra Pr} = 10^{24}$, the solar luminosity $L = L_\odot$ is reached

Ra Pr	u_t	Ma	L/L_\odot
10^6	20 km/s	10^{-1}	10^9
10^{12}	2 km/s	10^{-2}	10^6
10^{24}	20 m/s	10^{-4}	1

The turbulent velocity u_t is a slowly *decreasing* function of Ra. Realistic models of the lower part of the solar convection zone can only be obtained when Ra Pr is of the order 10^{24} (Ra of the order 10^{30}). If Ra was too small, $\bar{\chi}$ would be too large, and the radiative flux that enters from below would be too large for a realistic temperature gradient. Consequently, in order to model realistically the deep solar convection zone, subgrid-scale diffusivities have to be employed to stabilise the scheme whilst reducing $\bar{\chi}$ to realistically small values.

3 Magnetic Field Loops and Bipolar Regions

Even though in our simulations the magnetic field is unrealistically weak, there is a clear tendency for the formation of bipolar regions. An example of such an event is shown in Fig. 1, where we plot magnetic field vectors for a simulation with an imposed horizontal magnetic field with $B_0 = 0.06 B_{\text{eq}}$, in the presence of rotation (the inverse Rossby number is $\text{Ro}^{-1} \equiv 2\Omega d/u_t = 1.6$), the magnetic Reynolds number $R_m \equiv u_t d/\eta = 120$, and the resolution $63 \times 63 \times 37$ mesh points (Brandenburg et al. 1993b).

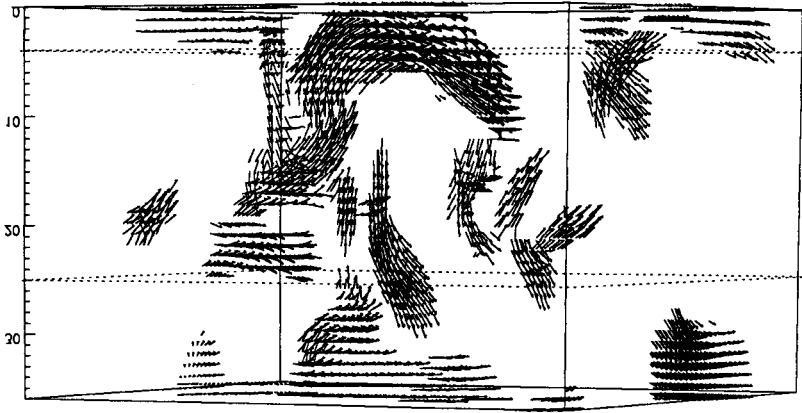


Fig. 1. Magnetic field vectors in a simulation with an imposed magnetic field B_0 in the x -direction (from the left to the right on the paper). Note the formation of a big loop producing a bipolar region at the upper surface. The boundaries of the unstable region are marked by dotted lines

It turns out that bipolar regions are often aligned with the direction of the mean magnetic field, even though it is rather weak compared with the field in typical flux tubes. The large scale magnetic field is usually strongest in the lower overshoot layer. Due to persistent pumping of magnetic field into this layer, the magnetic field is able to accumulate here (Brandenburg et al. 1991a, Rüdiger & Kitchatinov 1992, Petrovay & Szakály 1993). In the present simulations the field is still rather irregular in the overshoot layer, but it is conceivable that under more realistic circumstances the turbulent time scales are much longer in this layer, thus giving enough time for individual flux tubes to line up with the large scale field.

4 Development of Large Scale Fields

Following the pioneering work of Frisch et al. (1975) and Pouquet et al. (1976), a large scale magnetic field is generated in the presence of either magnetic or kinetic helicity by an inverse cascade of the magnetic helicity which, in turn, gives rise to an inverse cascade of the magnetic energy. This leads to a build-up of the magnetic field at large scales. This effect is also seen in simulations of a convective dynamo action. In Fig. 2 we plot the magnetic energy spectrum $M(k)$ for two different times (approximately 10 turnover times apart) for a run with $R_m = 1000$, $Ro^{-1} = 1$, at a resolution of 63^3 mesh points (Nordlund et al. 1992).

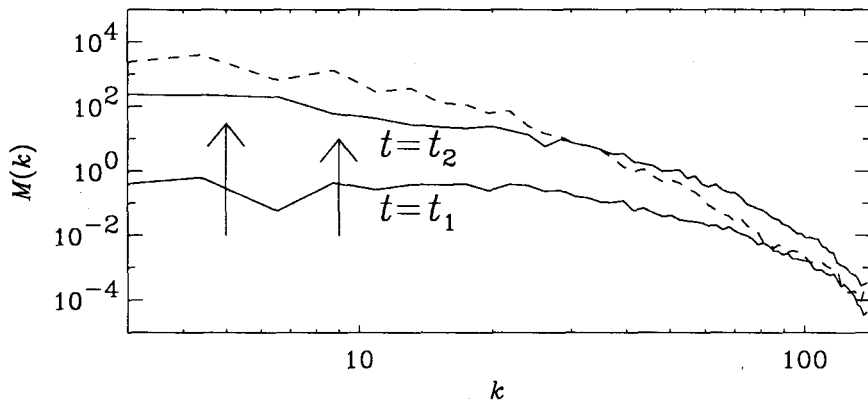


Fig. 2. Magnetic energy spectra during the growth phase ($t = t_1$) and the saturated phase ($t = t_2$) of a dynamo (lower and upper solid curve). For comparison, the kinetic energy spectrum at $t = t_2$ is also shown (dotted line)

The α -effect formalism of Steenbeck, Krause & Rädler (1966) may be considered as a linearised version of the fully nonlinear approach mentioned above. In Fig. 3 we show that a simple, one-dimensional, α^2 -dynamo gives rise to an inverse cascade, similar to the inverse cascade in MHD turbulence. This is illustrated in the second panel of Fig. 3, where we show a sequence of magnetic energy spectra from a simple cascade model of convective MHD turbulence (Brandenburg 1992). The main difference is that in the α -effect dynamo the growth of magnetic energy at small scales is not described.

The difference in the form of the magnetic energy spectra during the growth phase of the dynamo and during the saturated phase is an important property. The development of small scale structures is an inherently kinematic process: as time goes on, larger and larger structures develop. This is also seen by comparing snapshots of simulations: during the growth phase of the dynamo the flux tubes are thinner than at later times when the flux tubes become more clearly defined (Brandenburg et al. 1991b).

5 Intermittency and Small Scale Fields

It has been argued that magnetic fluctuations that are very strong compared to the large scale magnetic field can lead to a severe quenching of the α -effect and the turbulent magnetic diffusivity (Vainshtein & Cattaneo 1992). The fluctuating magnetic field is considered strong enough when the ratio $q \equiv \langle B^2 \rangle / \langle B \rangle^2$ is of the order of R_m . This would be the case if the magnetic energy spectrum had an inertial

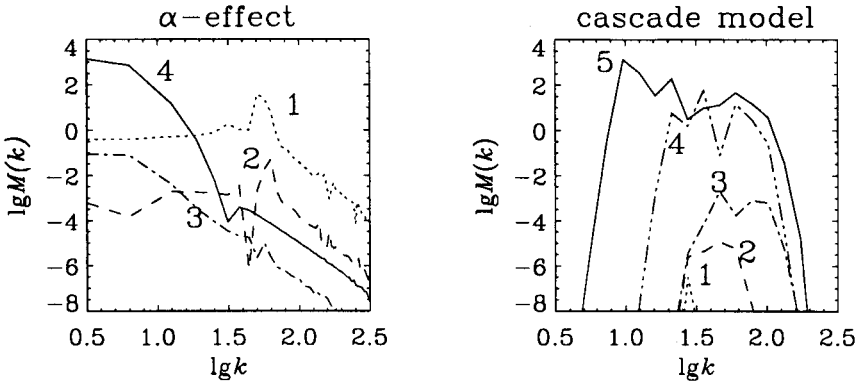


Fig. 3. Magnetic energy spectra of a one-dimensional α -effect dynamo (left panel) and a simple cascade model of MHD turbulence (right panel). The numbers on the curves indicate increasing time

range that increases like $k^{+1/3}$ with wave number k (Moffatt 1961). By contrast, if the magnetic energy had for example a k^{-1} spectrum, q would asymptotically only increase like $\ln R_m$ (Zeldovich et al. 1983, Kleeorin et al. 1990). Furthermore, as the mean magnetic field strength increases, the quantity q is quenched and becomes of order unity as $|\langle \mathbf{B} \rangle| \rightarrow B_{\text{eq}}$ (Kleeorin et al. 1990, Brandenburg et al. 1993b). In other words, it is possible that the magnetic fluctuations are of comparable order of magnitude to the mean magnetic field.

It is important to note that the quantity $\langle B^2 \rangle$ can be significantly underestimated if the magnetic field continues to be intermittent and nonsmooth down to the smallest scales resolved. This is a particular problem when observational data are analysed. It is sometimes possible to extrapolate to the limit of perfect resolution by measuring the moments of the average magnetic field at different resolution,

$$\mathcal{B}_n(r) = \langle (|\langle \mathbf{B} \rangle_r|^n) \rangle. \quad (3)$$

Here, $\langle \dots \rangle_r$ denotes an average over a box of scale r , and $\langle \dots \rangle$ is an average over the entire computational volume. The function $\mathcal{B}_2(r)$ is closely related to the magnetic energy spectrum. As an example we show in Fig. 4 the scaling of $\mathcal{B}_n(r)$ for data from a numerical simulation with $\text{Ra} = 10^6$, $\text{Pr} \equiv \nu/\bar{\chi} = 0.2$, and $\text{Pr}_M \equiv \nu/\eta = 4$ (Nordlund et al. 1992).

Note that in the lin-log plot (Fig. 4) the curves are almost straight lines at small scales of r , which is related to an exponential power spectrum of the magnetic energy in the dissipation range. This suggests that it is possible to extrapolate to $r = 0$. For example, at the smallest resolved scale, $r_0 = 1$ mesh size, $\mathcal{B}_2(r_0)$ is $4.7 \cdot 10^{-4}$, but the extrapolated value $\mathcal{B}_2(0)$ increases to about $6.4 \cdot 10^{-4}$. In the present case we have $q \approx \mathcal{B}_2(0)/\mathcal{B}_2(32r_0) = 350$. Since the average magnetic field over the entire box vanishes due to boundary and initial conditions, this ratio depends strongly on

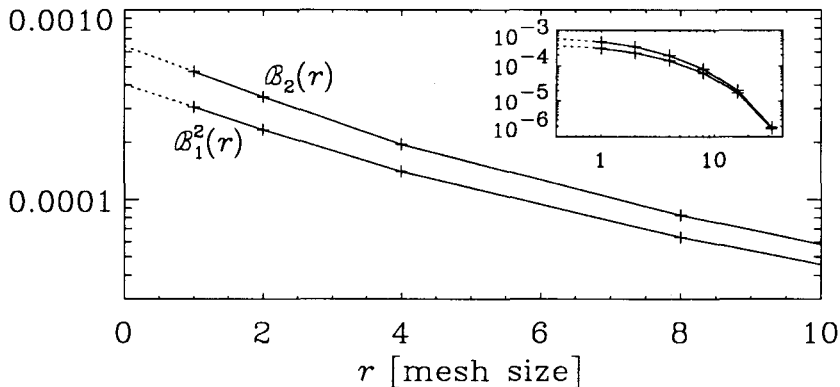


Fig. 4. $\mathcal{B}_2(r)$ and $\mathcal{B}_1^2(r)$ for data of a numerical simulation with dynamo effect. (In the plot, the square of $\mathcal{B}_1(r)$ is shown to allow comparison with $\mathcal{B}_2(r)$.) $Ra = 10^6$, $Pr = 0.2$, and $Pr_M = 4$. The inset shows a log-log plot of the same data

the scale at which the denominator is evaluated. For example at half the scale this ratio is much smaller: $\mathcal{B}_2(0)/\mathcal{B}_2(16r_0) = 32$.

The slope $\kappa = d \ln \mathcal{B}_1 / d \ln r$, evaluated at the skin layer scale $r \sim LR_m^{-1/2}$, is the cancellation exponent (Ott et al. (1992, Bertozzi et al. 1993)). In the present case, where there is a small scale dynamo, this exponent is around 0.2. A nonvanishing exponent indicates that the field is still “rough” down to the smallest scale resolved. There is however no power law behaviour, but instead $\mathcal{B}_n(r)$ is proportional to $\exp(-r/r_d)$ with $r_d \approx 3r_0$ (for $n = 2$).

6 The α -Effect Evaluated from Simulations

The α -effect can in principle be evaluated from numerical simulations of convection (e.g. Brandenburg et al. 1990). Using such simulations one can compute α as a function of $|\langle \mathbf{B} \rangle|$. In the simulations of Brandenburg et al. (1993b), α seems to be surprisingly insensitive to $|\langle \mathbf{B} \rangle|$. Unfortunately it is not (yet?) possible to attain sufficiently large values of R_m , and it therefore remains open whether α is a sensitive function of the magnetic Reynolds number R_m . For example, $\alpha \sim R_m^{-1/2}$ has been obtained by Childress (1979) and Perkins & Zweibel (1989) for a model with a steady flow, and Vainshtein & Cattaneo (1992) argue that the onset of α -quenching occurs for progressively weaker fields as R_m increases. However, their argument requires $q = \mathcal{O}(R_m)$, implying a magnetic energy spectrum that increases towards larger k . This issue is still controversial, but it should be noted that there is evidence

that in the inertial range the magnetic spectrum does indeed decrease like k^{-1} (see discussion in Brandenburg et al. 1993b).

Another important application of such simulations is to determine the latitudinal dependence of α . Current theories (e.g. Rüdiger & Kitchatinov 1993) are restricted to only linear dependencies of α on $\hat{\mathbf{g}} \cdot \hat{\boldsymbol{\Omega}} \propto \cos \theta$, where $\hat{\mathbf{g}}$ symbolises the preferred direction due to a stratification of density or turbulent intensity, and θ is colatitude. In Fig. 5 we show the longitudinal (ϕ -) component of α , $\langle \mathbf{u}' \times \mathbf{B}' \rangle_{\phi} / \langle B_{\phi} \rangle$, as a function of θ for two different values of Ro^{-1} .

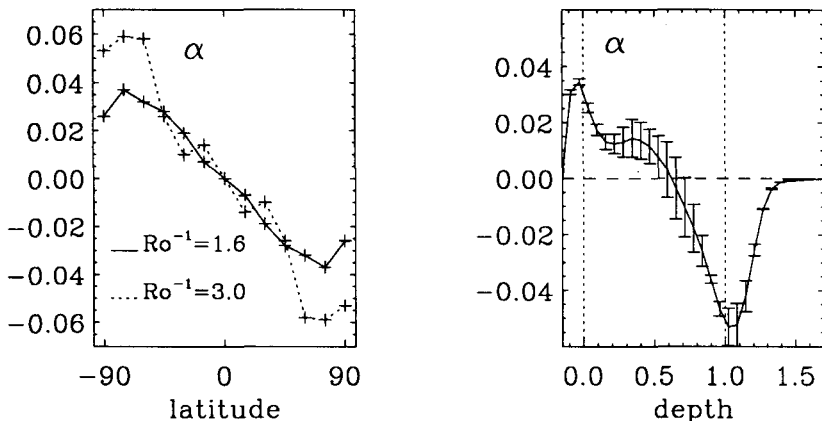


Fig. 5. *Left panel:* The latitudinal dependence of α for a simulation with $\text{Ra} = 310^5$ ($\text{Ro}^{-1} = 1.6$) and $\text{Ra} = 10^5$ ($\text{Ro}^{-1} = 3.0$). In all cases, $\text{Ta} = 310^4$, $\text{Pr} = 0.5$, and $\text{Pr}_M = 0.5$. *Right panel:* The depth dependence of α for the same parameters as before, but with $\text{Ro}^{-1} = 3.0$ and $\theta = 90^\circ$. The dotted vertical lines denote the boundaries of the convection zone

Note that α deviates from a simple $\cos \theta$ law. Indeed, there is no reason to expect such a simple dependence to be valid for strong stratification and rapid rotation, in which case higher powers in $\hat{\mathbf{g}} \cdot \hat{\boldsymbol{\Omega}}$ must occur in the α expressions. Rüdiger & Brandenburg (1993) used the empirical formula

$$\alpha(\theta) = \alpha_0 \cos \theta (1 - \alpha_U \cos^2 \theta). \quad (4)$$

with $\alpha_U \approx 1$ to model the solar dynamo in the overshoot layer. A similar latitudinal dependence of α has previously been suggested in order to explain a concentration of the sunspot activity maximum at low latitudes (Yoshimura 1975, Belvedere et al. 1991). Schmitt (1987) finds a similar dependence of a α -effect that is based on magnetostrophic waves.

There is another effect that can be seen in simulations in a spherical shell: inside the cylinder tangent to the inner radius of the shell the kinetic helicity is virtually zero for rapid rotation (e.g. Rieutord et al. 1993). It is not obvious whether this effect operates in the Sun, or whether it is an artifact of the simulations not being sufficiently turbulent.

In contrast to earlier estimates of α from convection simulations with weak stratification (Brandenburg et al. 1990), α now tends to be reduced in the bulk of the convection zone and concentrated towards the boundaries of the convection zone (Fig. 5). In any case, α is rather small and only a few percent of u_t . Whether or not mean-field dynamo action is possible with such a weak and localised α -effect depends crucially on the value of the turbulent magnetic diffusion, η_t . Theory predicts a decrease of η_t for large inverse Rossby numbers (Kitchatinov & Rüdiger 1993), and simulations also give values of η_t that are smaller than standard estimates.

The effect of η_t -quenching by the magnetic field has long been recognised (Roberts & Soward 1975). A severe suppression of η_t has been found in a special two-dimensional case (Cattaneo & Vainshtein 1991), but this does not seem to carry over into the three-dimensional regime (Nordlund et al. 1993). A suppression of η_t can be inferred from simulations by monitoring the decay rate of the large scale magnetic field component. For the convection simulations of Brandenburg et al. (1993b) we estimate $\eta_t \approx 0.2\eta_0$ for strong fields ($B \approx 0.2B_{\text{eq}}$), and $\eta_t \approx 0.4\eta_0$ for weak fields ($B \approx 0.006B_{\text{eq}}$), where $\eta_0 = \frac{1}{3}u_t d$ is a rough estimate for reference.

7 Mean-Field Dynamos

Using an α -effect of the form (4) with $\alpha_U = 1$, Rüdiger & Brandenburg (1993) computed mean-field dynamos for the overshoot layer beneath the solar convection zone, taking the full Rossby number dependence, the full α -tensor and the turbulent diffusivity into account (Rüdiger & Kitchatinov 1993). We already know from the Krause formula for α (Krause 1967) that α becomes negative at the bottom of the convection zone, because of the sharp gradient in the turbulent velocity. Beneath the interface of the convection zone and the radiative interior, the turbulent magnetic diffusivity gradually goes to zero. The magnetic field tends to accumulate in this interface; see Fig. 6.

Magnetic buoyancy acts mostly in the upper part of the convection zone, but it turns out that this effect can drastically increase the cycle period. Furthermore, due to the intermittent nature of the magnetic field, the effective electromotive force is reduced by a factor ϵ . For $\epsilon = 0.2 - 0.5$ the correct cycle period can be obtained.

All dynamo models with solar-like differential rotation ($\partial\Omega/\partial r > 0$ in the equatorial plane) have the common problem that at low latitudes poloidal and toroidal fields are in phase, which is in contrast to the observations. However, the indicators of these two field components probe different depths in the convection zone, and it is therefore plausible that the observed phase relation strongly depends on the depths where poloidal and toroidal fields are measured (B_r somewhere close to the surface and B_ϕ at the bottom of the convection zone). At intermediate and high latitudes, the poloidal and toroidal fields are in phase – in agreement with the solar field.

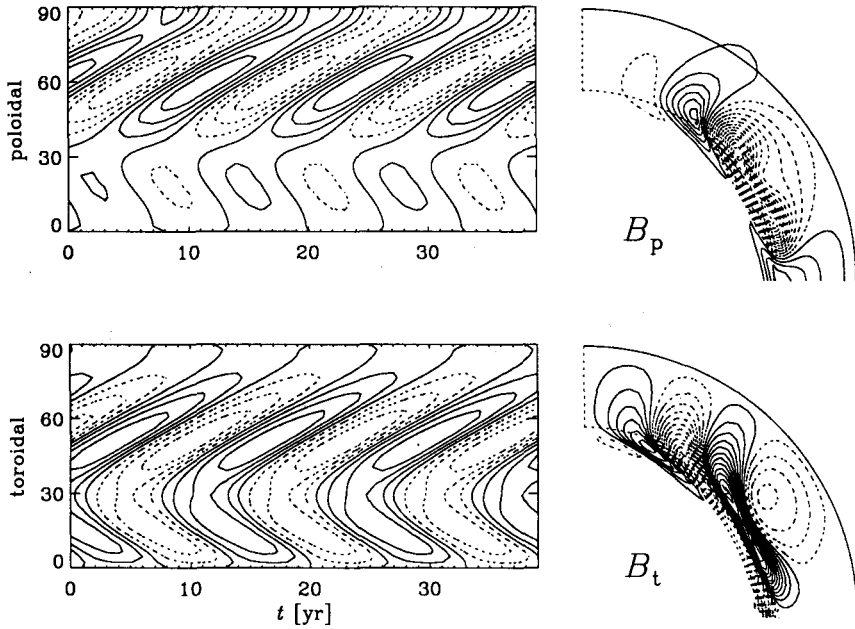


Fig. 6. Butterfly diagram for the B_r and the B_ϕ components of the mean magnetic field from a $\alpha\Omega$ -dynamo model for the Sun together with meridional cross-sections showing poloidal field lines and contours of the toroidal field

8 Discussion

Numerical simulations of MHD convection can help to improve significantly our understanding of solar and stellar magnetism. Such simulations suggest the possibility of dynamo action in the entire convection zone with field advection down to the bottom. Thus, whilst the magnetic field turns out to be strongest at this interface, the actual generation of the magnetic field in this layer is perhaps relatively unimportant.

This picture seems to be in contrast to the other possibility that most of the dynamo generation happens in the overshoot layer itself. The general problem with this approach is that in the overshoot layer the kinetic energy of the fluid motions is probably relatively weak and of the order of, or less than, the magnetic energy in that layer. Indeed, convective dynamo models presented so far typically generate magnetic fields whose strength does not significantly exceed the kinetic energy density of the turbulent motions that are generating this field. It seems therefore more

natural to generate magnetic field in the convection zone where the kinetic energy of the turbulent motions is large. Turbulent pumping and suction of the magnetic field by the intense downdrafts leads to an accumulation of the magnetic field at the interface, where the magnetic energy may then easily exceed the kinetic energy of the motions.

A systematic large scale magnetic field is expected to occur in deeper regions where the motions are slow enough. The dynamo process seen in numerical simulations generates a small scale magnetic field that consists of a number of intense flux tubes. Future mean-field models of the solar magnetic field should therefore incorporate such small scale fields which, in principle, may play an active role in the formation of large scale fields via inverse cascade type mechanisms. Future simulations, on the other hand, should be carried out in larger boxes that include effects of the spherical geometry of the Sun.

References

- Belvedere, G., Proctor, M. R. E., Lanzafame, G. (1991): "The latitude belts of solar activity as a consequence of a boundary-layer dynamo", *Nature* **350**, 481-483
- Bertozzi, A. L., Chhabra, A. B., Kadanoff, L. P., Ott, E., Vainshtein, S. I. (1993): On dynamo generation of magnetic flux and fractal properties of the field. (preprint).
- Brandenburg, A. (1992): "Energy spectra in a model for convective turbulence", *Phys. Rev. Lett.* **69**, 605-608
- Brandenburg, A., Nordlund, Å., Pulkkinen, P., Stein, R.F., Tuominen, I. (1990): "3-D Simulation of turbulent cyclonic magneto-convection", *Astron. Astrophys.* **232**, 277-291
- Brandenburg, A., Jennings, R. L., Nordlund, Å., Stein, R. F., Tuominen, I. (1991a): The role of overshoot in solar activity: A direct simulation of the dynamo in The Sun and cool stars: activity, magnetism, dynamos, ed. by I. Tuominen, D. Moss & G. Rüdiger (Lecture Notes in Physics **380**, Springer-Verlag) pp.86-88
- Brandenburg, A., Jennings, R. L., Nordlund, Å., Stein, R.F. (1991b): Magnetic flux tubes as coherent structures in Spontaneous formation of space-time structures and criticality, ed. by T. Riste & D. Sherrington (Nato ASI Series) pp.371-374
- Brandenburg, A., Jennings, R. L., Nordlund, Å., Rieutord, M., Stein, R. F., Tuominen, I. 1993a Magnetic structures in a dynamo simulation. *J. Fluid Mech.* (submitted).
- Brandenburg, A., Krause, F., Nordlund, Å., Ruzmaikin, A. A., Stein, R.F., Tuominen, I. 1993b On the magnetic fluctuations produced by a large scale magnetic field. *Astro-phys. J.* (submitted).
- Cattaneo, F., Vainshtein, S. I. (1991): "Suppression of turbulent transport by a weak magnetic field", *Astro-phys. J.* **376**, L21-L24
- Childress, S. (1979): "Alpha-effect in flux ropes and sheets", *Phys. Earth Planet. Int.* **20**, 172-180
- Frisch, U., Pouquet, A., Léorat, J., Mazure, A. (1975): "Possibility of an inverse cascade of magnetic helicity in hydrodynamic turbulence", *J. Fluid Mech.* **68**, 769-778
- Kitchatinov, L. L., Rüdiger, G. (1992): "Magnetic-field advection in inhomogeneous turbulence", *Astron. Astrophys.* **260**, 494-498
- Kitchatinov, L. L. & Rüdiger, G. (1993): (in preparation)
- Krause, F. (1967): *Eine Lösung des Dynamoproblems auf der Grundlage einer linearen Theorie der magnetohydrodynamischen Turbulenz*, (Habilitationsschrift, University of Jena)

- Krause, F., Rädler, K.-H. (1980): *Mean-Field Magnetohydrodynamics and Dynamo Theory*, (Akademie-Verlag, Berlin)
- Kleorin, N. I., Rogachevskii, I. V., Ruzmaikin, A. A. (1990): "Magnetic force reversal and instability in a plasma with advanced magnetohydrodynamic turbulence", *Sov. Phys. JETP* **70**, 878–883
- Küker, M., Rüdiger, G., Kitchatinov, L. L. 1993 An $\alpha\Omega$ -model of the solar differential rotation. *Astron. Astrophys.* (in press).
- Moffatt, H. K. (1961): "The amplification of a weak magnetic applied magnetic field by turbulence in fluids of moderate conductivity", *J. Fluid Mech.* **11**, 625–635
- Nordlund, Å., Brandenburg, A., Jennings, R. L., Rieutord, M., Ruokolainen, J., Stein, R. F., Tuominen, I. (1992): "Dynamo action in stratified convection with overshoot", *Astrophys. J.* **392**, 647–652
- Nordlund, Å. et al. (1993): (in preparation)
- Ott, E., Du, Y., Sreenivasan, K. R., Juneja, A. & Suri, A. K. (1992): "Sign-singular measures: fast magnetic dynamos, and high-Reynolds-number fluid turbulence", *Phys. Rev. Lett.* **69**, 2654–2657
- Perkins, F. W., Zweibel, E. G. (1987): "A high magnetic Reynolds number dynamo", *Phys. Fluids* **30**, 1079–1084
- Petrovay, K., Szakály, G. (1993): "The origin of intranetwork fields: a small-scale solar dynamo", *Astron. Astrophys.* **274**, 543–554
- Pouquet, A., Frisch, U., Léorat, J. (1976): "Strong MHD helical turbulence and the nonlinear dynamo effect", *J. Fluid Mech.* **77**, 321–354
- Rieutord, M. et al. 1993 Reynolds stress and differential rotation in Boussinesq convection in a rotating spherical shell. *Astron. Astrophys.* (to be submitted).
- Roberts, P. H., Soward, A. M. (1975): "A unified approach to mean field electrodynamics", *Astron. Nachr.* **296**, 49–64
- Rüdiger, G., Kitchatinov, L. L. (1993): "Alpha-effect and alpha-queenching", *Astron. Astrophys.* **269**, 581–588
- Rüdiger, G., Brandenburg, A. 1993 A solar dynamo in the overshoot layer: cycle period and butterfly diagram. *Astrophys. J.* (submitted).
- Schmitt, D. (1987): "An $\alpha\omega$ -dynamo with an α -effect due to magnetostrophic waves", *Astron. Astrophys.* **174**, 281–287
- Schmitt, D. (1993): (this volume)
- Steenbeck, M., Krause, F., Rädler, K.-H. (1966): "Berechnung der mittleren Lorentz-Feldstärke $\overline{\mathbf{v} \times \mathbf{B}}$ für ein elektrisch leitendes Medium in turbulenter, durch Coriolis-Kräfte beeinflusster Bewegung", *Z. Naturforsch.* **21a**, 369–376
- Vainshtein, S. I., Cattaneo, F. (1992): "Nonlinear restrictions on dynamo action", *Astrophys. J.* **393**, 165–171
- Yoshimura, H. (1975): "A model of the solar cycle driven by the dynamo action of the global convection in the solar convection zone", *Astrophys. J. Suppl.* **29**, 467–494
- Zeldovich, Ya. B., Ruzmaikin, A. A., Sokoloff, D. D. (1983): *Magnetic fields in Astrophysics*, (Gordon & Breach, New York)